Journal of Earth Sciences 2 (2016) 94-104 **Betty Jones & Sisters Publishing**
ISSN 2372-5176 **http://www.bettyjonespub.com**

Nano-sized Iron-oxides in the Dead Sea area

Nurit Taitel-Goldman[1], Vladimir Ezersky[2], Dmitry Mogilyanski[2]

1. The Open University P.O. Box 808 Raanana, Israel 4353701

2. Ilse Katz Institute for Nanoscale Science and Technology, Ben-Gurion University of the Negev, Beer-Sheva, Israel 8410501

Abstract: Iron-oxides precipitated from discharging Ca-Chloride hyper-saline brines close to the Dead Sea or from the Ein Ashlag spring located on the eastern flanks of the Mount Sedom diapir. Initially formed iron-oxides precipitated on several surfaces and were later preserved within halite crystals, hence recrystallization processes were hindered. The iron-oxides were identified by using XRD and High resolution transmission electron microscopy (HRTEM). The initially formed phase is short-range ordered ferrihydrite (Fe5HO8*4H2O) with Si/Fe = 0.05-0.26, Mn/Fe = 0.02-0.06 and P/Fe = 0.02 impurities. Goethite (α FeOOH) had an acicular and multi-domain morphology with an Mn impurity forming a solid solution goethite-groutite due to similar ionic radii. Recrystallization processes of goethite in Ein Ashlag led to more pure phases. Akaganéite (β FeOOH) preserved the morphology of the ferrihydrite precursor and had Si (Si/Fe= 0.05) and Mn impurities (Mn/Fe = 0.02-0.06). Recrystallization processes yielded a rod-shaped akaganéite. Lepidocrocite (γ FeOOH) crystallized at a relatively fast oxidation rate, and had Si and Mn impurities that reached the values of Si/Fe = 0.06 and Mn/Fe = 0.06. Tiny hematite (α Fe2O3) crystallites were found in a recently-formed crust covering limestone pebbles close to a discharging spring. Hematite morphology indicates that it was formed by dehydration and rearrangement of the ferrihydrite precursor and the initial morphology was preserved.

Key words: Dead-Sea, ferrihydrite, goethite, akaganéite, lepidocrocite, hematite

1. Introduction

The hyper-saline terminate lake of the Dead Sea is located along the Dead Sea transform fault. The salinity of the lake reaches 340g/l [1] and has a Ca-Chlorides composition that results from a few stages: a) an elevated concentration due to evaporation in a marine lagoon that was connected to ancient Mediterranean seawater by an inland channel; b) water-rock interaction with surrounding Upper Cretaceous limestone and the forming of epigenetic discordant dolomite led to its losing most of its Mg^{2+} and gaining Ca^{2+}; c) the mixing with freshwater or other saline water and removal of SO_4^{2-} and HCO_3^- imported to the lake by precipitation of $CaCO_3$ and $CaSO_4$ minerals [1-2]. Three aquifers interact with the Dead Sea water: the quaternary alluvial aquifer, the Upper Cretaceous carbonate Judean aquifer, and the Lower Cretaceous Kurnubs and stone aquifer.

Circulation of the Dead Sea hyper-saline brine in the aquifer leads to the dissolution of Fe and Mn oxides due to reducing conditions. Hence, the Fe concentration increases from 1 mg/l in the Dead Sea water to 19 mg/l in close boreholes. Mn concentration in the Dead Sea water is 7 mg/l and it reaches 9.4 mg/l in boreholes [3].

Over the last decades, the sea level of the Dead Sea has dropped to a water level of ~420m below sea level, hence salt stones that had precipitated earlier from the brine are now exposed, and saline brine springs discharge at the area. The emergence of surrounding springs at the Dead Sea area results from: a) a flow of meteoric water in the regional aquifer; b) compaction of the strata due to tectonic movement; c) an eastward flow of the meteoric water that forces deep water brines towards the Dead Sea valley; d) the force of the Dead

This research was supported by the Open University of Israel, Grant no. 100975.

Corresponding author: Nurit Taitel-Goldman, Ph.D., research fields: formation of iron oxides, in hydrothermal and hyper-saline environments. E-mail: nuritg@openu.ac.il

Sea deep water brines to the surface by the pressure of the Dead Sea water body [1].

Ein Ashlag is a hyper-saline seepage issuing from the northeast corner of the Mt. Sedom salt diapir. Chemical composition of the Ein Ashlag spring water is TDS 391 g/l Cl-260g/l Fe^{2+} 0.12g/l, Mn 0.04 g/l, and pH 5 measurements of the Dead Sea water yielded TDS 340g/l Cl 226 g/l and pH 5.3-6.1 [4].

The aims of this research are to study nano-sized iron-oxides that are initially formed in the hyper-saline environment. Some of the crystals were preserved within halite crystals, hence it is possible to follow recrystallization processes in this hyper-saline environment.

2. Location and Methods

Two main sites were sampled for this study. Samples were collected from the area between the Dead Sea and the evaporation ponds that earlier were part of the Dead Sea and today are separated from the main lake (Figures 1a, 1b, 1c).Various phases of iron-oxides form inclusions in halite crystals and lead to colored areas (Figure 1d) and colored halite crystals (Figure 1f). Iron-oxides coat pebbles in a channel close to the discharging spring (Figure 1h). The second site is near the Ein Ashlag spring, located at the eastern part of the Sedom salt diapir (Figure 1e), and iron-oxides precipitate along the river bed (Figure 1g), (Table 1).

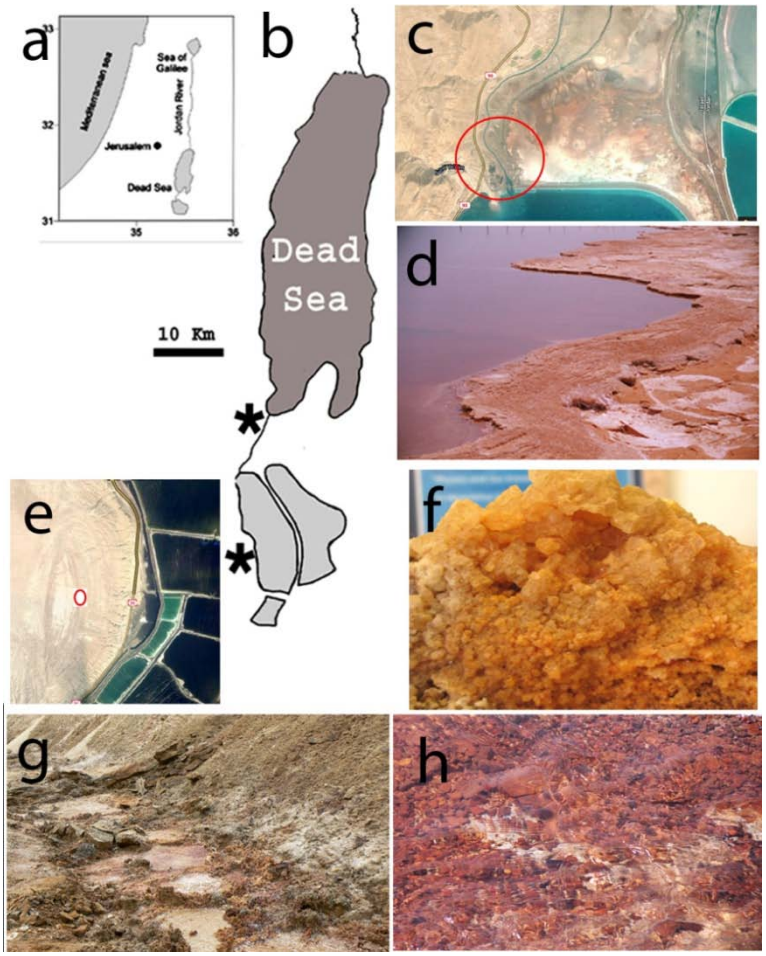

Fig. 1 a) Map of the area; b) Location of two sampling sites near the Dead Sea; c) Aerial map of the sampling area near the northern evaporation pond (red circle); d) Sampling area close to the northern evaporation pond; e) Aerial view of the Sedom diapir and the Ein Ashlag location (red circle); f) Halite crystals with iron-oxides inclusions; g) The Ein Ashlag spring riverbed; h) pebbles coated with iron-oxides in a channel.

Table 1 Sample location and iron-oxides identified Chemical analyses of the discharging brines were obtained by ICP-MS; Cl concentration was obtained by titration.

Sample no.	Location	Iron oxides
DS-1	Salt from 1st pond	ferrihydrite, akaganéite
DS-2	Salt from 1st pond	ferrihydrite
DS-3	Salt + brine near waterfall	akaganéite
DS-4	Layered sediment near 1st pond	ferrihydrite, goethite
DS-5	Upper red crust in a stream above gray mud	ferrihydrite
DS-6	Yellow red crust in a stream	ferrihydrite
DS-7	Plastic bag covered with red material	ferrihydrite
DS-8	Crust in a stream	ferrihydrite, hematite
DS-9	Crystalline salt	goethite, solid solution goethite-groutite,
DS-10	Crystalline crust near stalactites	lepidocrocite
DS-11	38.5ºC brine in a stream	
DS-12	Pebbles covered with crust within a stream	
DS-13	27.5ºC brine discharge	
DS-14	Crusts of iron oxides near the discharging brine	ferrihydrite
EA 6	3 m from discharging spring	akaganéite, goethite
EA 9	10 m from discharging spring	akaganéite, goethite

Salt was removed from the samples by distilled water and the insoluble residue was frozen and dried. The fine fractions, namely, clay-sized particles obtained were analyzed using Philips 1050 X-ray diffractometer CuKα radiation, a curved-graphite diffracted–beam monochromator, a step size of 0.02°2θ, a counting time of 2 s per step and 10% NBS640-silicon added as an internal standard.

Nano-sized (5-200 nm) particles were checked with High Resolution Transmission Electron Microscopy (HRTEM) using a JEOL FasTEM 2010 electron microscope equipped with a Noran energy dispersive spectrometer (EDS) for microprobe elemental analyses. All chemical analyses were obtained by point analyses with a beam width of 25 nm and are presented as atomic ratios. A NORAN Standard less metallurgical thin films program based on the Cliff-Lorimer ratio technique with an accuracy of ~5% was used for the calculations. The CuKa line was used to calibrate the spectrometer. Crystalline phases were identified, using selected area electron diffraction (SAED) in the TEM. With this method, a very high-energy electron beam (200 kV) transmits through the sample and the d- values obtained enabled their identification. The accuracy of the d- values determination was better than 0.005 nm. The smallest area of SAED was 100 nm. If a good lattice image was obtained in very small particles, the use of Fast Fourier transformation (FFT) enabled the identification of the minerals, using the program Digital Micrograph (Gatan).

3. Results and Discussion

3.1 Chemical Analyses of Discharging Brines

The temperatures of the springs yielded similar values. The temperature measured in the channel was similar to the air temperature.

Table 2 Chemistry and temperatures of Dead Sea area brines.

Sample	Location	Temp.°C	Cl (g/l)	Na (g/l)	Fe (mg/l)	Mn (mg/l)	Si (mg/l)
DS 3	Brine near a waterfall			9.5	74.3	1.45	0.09
DS 11	Flowing water in a channel	38.5		23.9	58.74	0.48	0.3
DS 13	Discharging brine close to the channel	27.5		22.4	34.9	0.6	0.25
EA 5	Discharging brine at Ein Ashlag	27.7	257	17.8		33.4	5.7
EA 8	5 m from the discharging brine		257	20.7		42.7	6.5
EA 10	10 m from the discharging brine		239	17.8		40.9	7.7

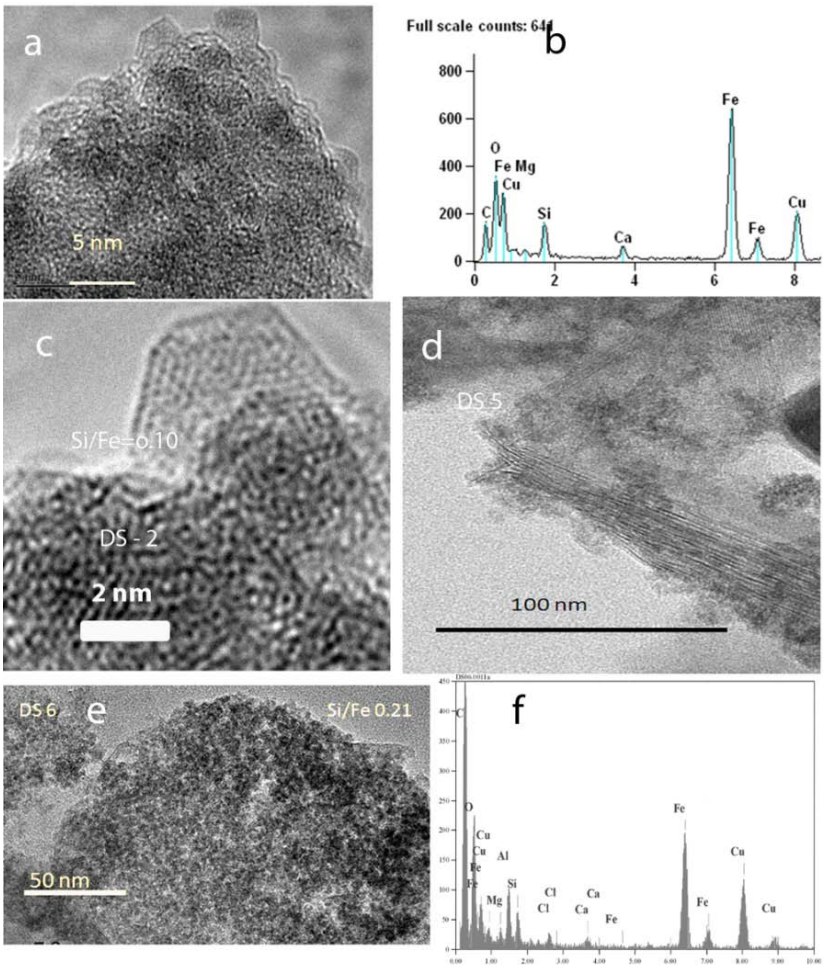

Fig. 2 Ferrihydrite from samples at the Dead Sea area. a, b) Ferrihydrite coating a plastic bag floating in a pool and point analyses of the crystallites; c) Ferrihydrite preserved within halite crystals; d) A ferrihydrite cluster that precipitated on a riverbed close to clay minerals; e, f) Ferrihydrite coating pebbles and impurities obtained by point analyses.

3.2 Ferrihydrite $Fe_5HO_8*4H_2O$

The initial stage of iron-oxides that precipitate in the area is short-range ordered nano-sized ferrihydrite (2-5 nm). Some of the initially formed ferrihydrite crystallites were found coating a plastic bag, floating in a small pool close to the discharging brine (Figure 2a). Impurities obtained by point analyses were Si (Si/Fe

= 0.27), Ca (Ca/Fe = 0.08) and Mg (Mg/Fe = 0.07) (Fig. 2b). Other ferrihydrite crystallites that were preserved within halite crystals (Fig. 2c) had impurities of Si (Si/Fe = 0.105), Mn (Mn/Fe = 0.013) and P (P/Fe = 0.023). Ferrihydrite that precipitated on the riverbed close to the discharging brine (Fig. 2d) and the coating pebbles in the pool had impurities of Si (Si/Fe = 0.21) and Ca, Mg in small amounts (Fig. 2e, 2f). Ferrihydrite usually precipitates at fast oxidation, pH < 5 and the presence of Si that hinders better crystallization leads to the formation of a short-range ordered phase and small crystallites. Other impurities within ferrihydrite crystallites result from water composition of the discharging spring and particles of dust.

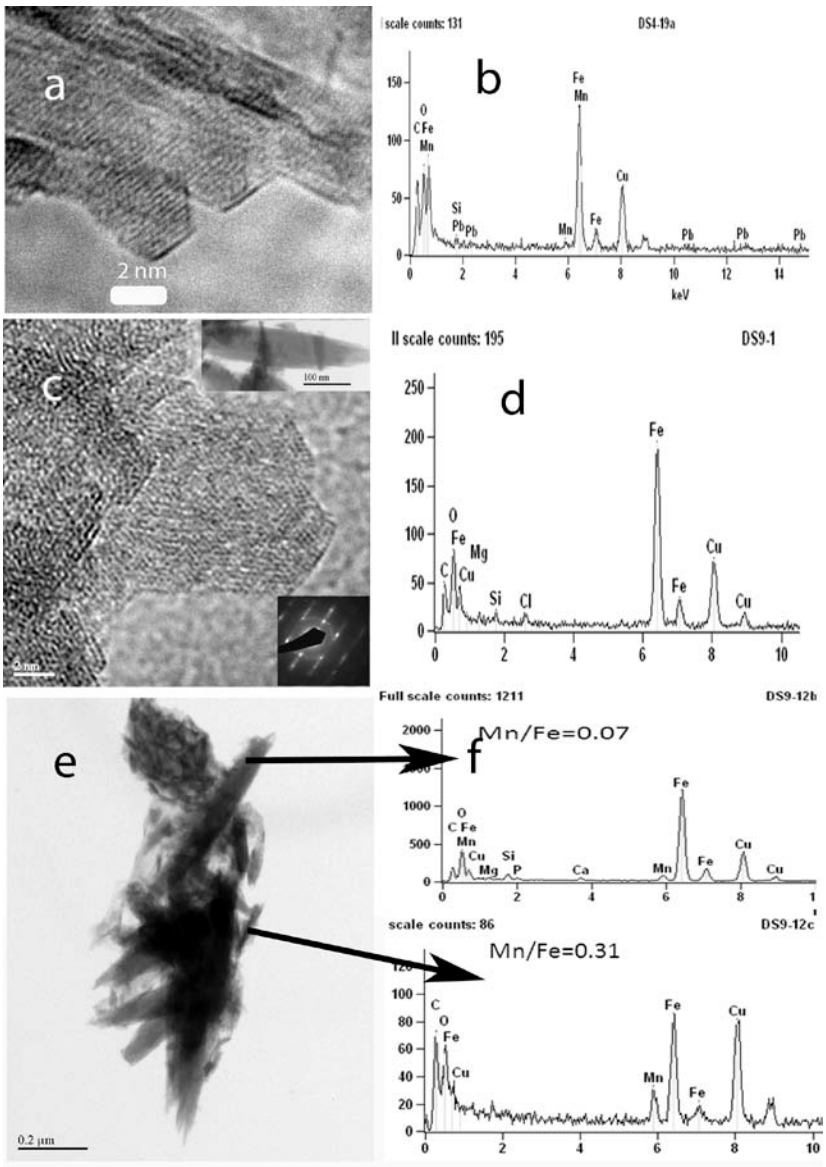

Fig. 3 Goethite samples from the Dead Sea area; a, b) A high resolution image of multi-domain goethite preserved within halite crystals with point analyses; c, d) Large multi-domain goethite crystals with electron diffraction high and point analyses; e) A cluster of goethite and solid solution of goethite-groutite with point analyses.

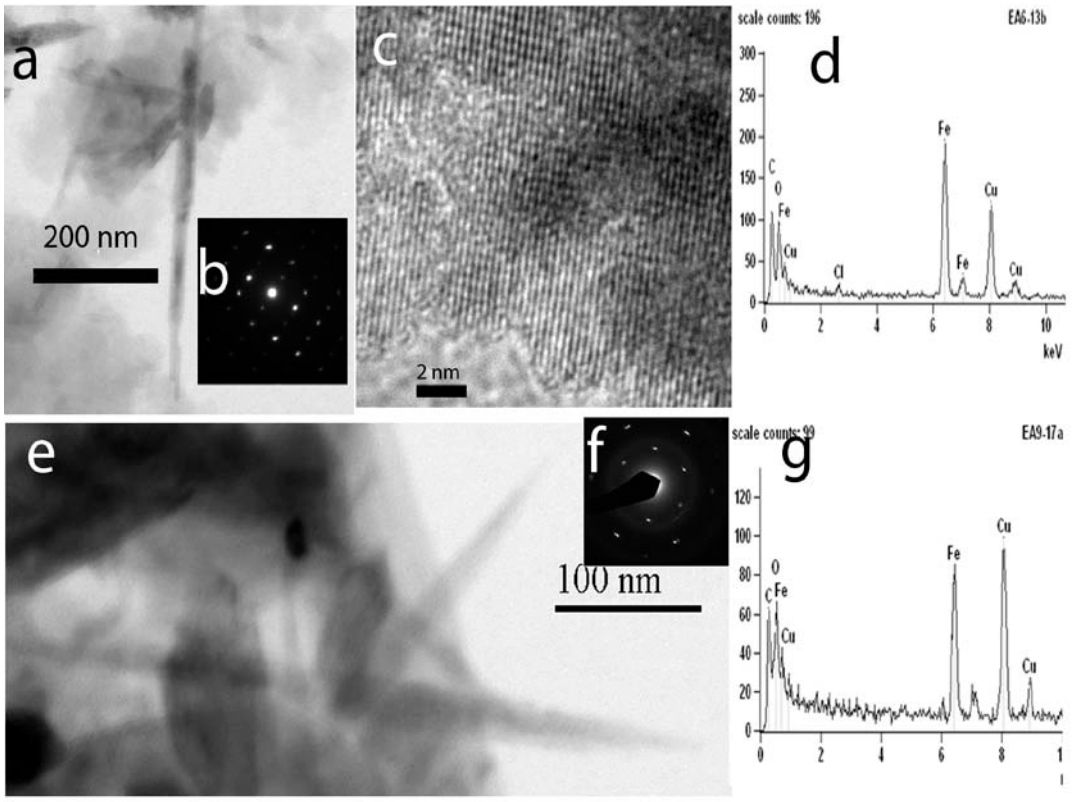

Fig. 4 Multi-domain goethite from Ein Ashlag. a-d) An image of multi-domain goethite 3 m from the Ein Ashlag spring with electron diffraction, a high resolution image and point analysis; e-g) Multi-domain goethite 10 m from the Ein Ashlag spring with electron diffraction and point analysis.

3.3 Goethite -α FeOOH

Multi-domain goethite crystallites that were preserved within halite crystals reached the length of a few hundred nm and the width of each domain was 2-3 nm. The impurities detected were Si (Si/Fe=0.08), Mn (Mn/Fe = 0.04) and Pb (Pb/Fe = 0.01) (Figure 3a, 3b, 3c, 3d). Multi-domainic structure is promoted by high ionic strength and mainly-elevated Na concentration and temperatures < 40°C [5-6]. The cluster of goethite crystals preserved within halite crystals had an elevated ratio of Mn/Fe = 0.31, indicating a possible solid solution goethite–grouthite (MnOOH) (Figure 3e, 3f) due to similar ionic radii Fe^{3+}-0.0645 nm Mn^{3+}-0.0645 nm and having the same similar structure (Orthorhombic – Dipyramidal H-M Symbol (2/m 2/m 2/m) Space Group: Pbnm). Chemically pure elongated multi-domain crystals of goethite were found 3 m and 10 m from the discharging spring of Ein Ashlag preserved within halite crystals (Figure 4). The size of the crystals reached 300nm and twinning was observed in the more distant sample. Remnants of a ferrihydrite precursor were observed in a goethite high resolution electron micrograph that was sampled close to the discharging spring.

3.4 Akaganéite - β FeOOH

Rod-shaped akaganéite were observed within halite crystals ~100nm long with a width of~ 10nm. The main impurities were Si (Si/Fe = 0.06-0.1), Cl (Cl/Fe = 0.07-0.12), Mn (Mn/Fe = 0.02-0.06) and small amounts of Na, and Mg probably originating from the brines (Figure 5a, 5b) Akaganéite crystals had an acicular character (Figure 5c) and the high resolution image shows a well-crystallized pattern (Figure 5d).

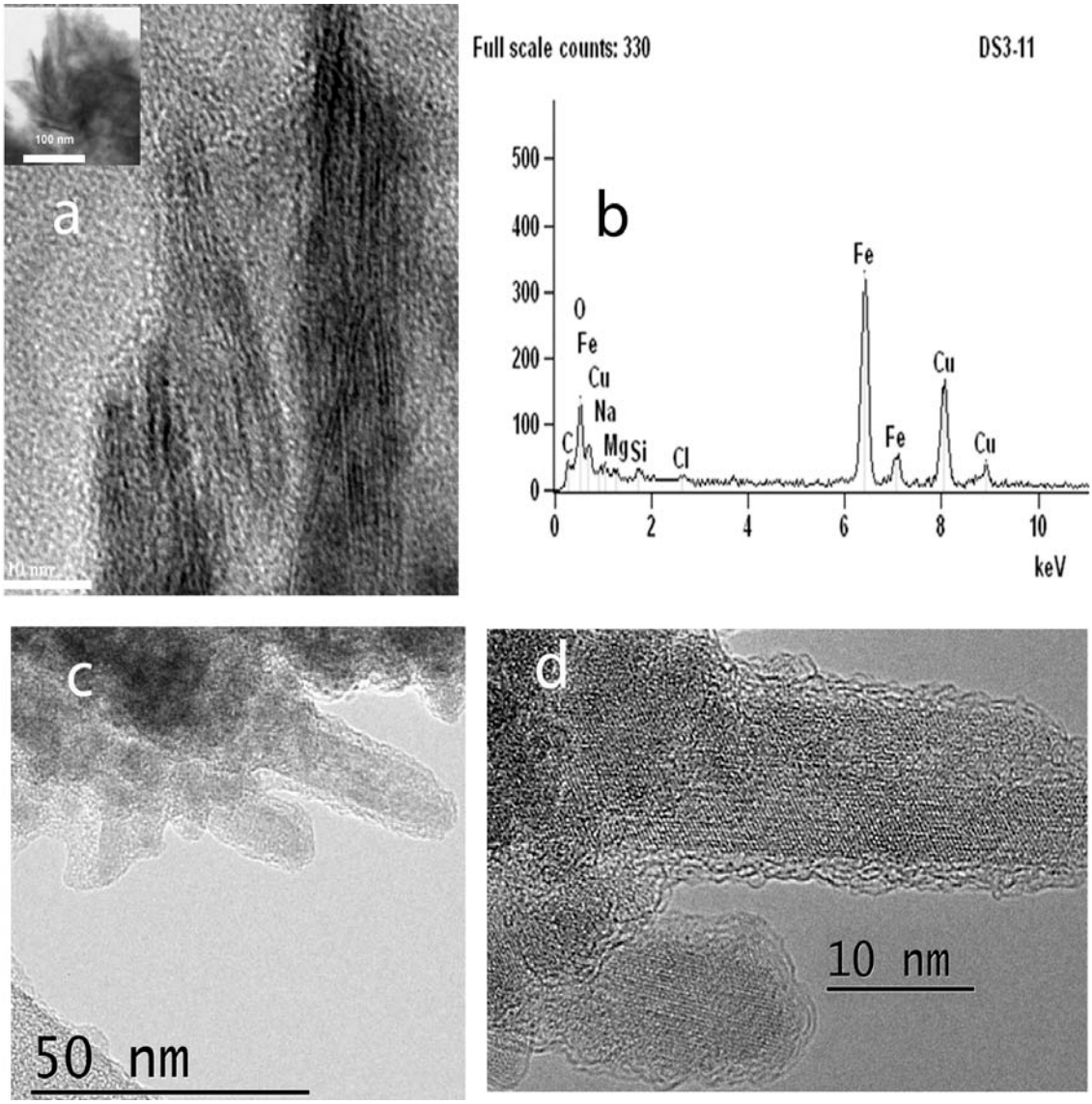

Fig. 5 Akaganéite from the Dead Sea area, a) A high resolution image of akaganéite forming cluster of crystals (the upper part of the image; b) A point analysis of akaganéite with impurities; c-d) Rod-shaped akaganéite in high resolution images.

Two morphologies of akaganéite were found close to the Ein Ashlag spring. Three m from the discharging spring, akaganéite preserved the morphology of the ferrihydrite precursor (Figure 6a) and had impurities of Si (Si/Fe = 0.05), Ca (Ca/Fe = 0.01) and Al (Al/Fe = 0.01), probably due to remnants from the ferrihydrite and small amounts of clays. 10 m away from the spring, elongated rods of akaganéite were observed (Figure 6b), probably due to cycles of dissolution and reprecipitation close to the flowing spring. Impurities found within the crystals were Si (Si/Fe = 0.04) and Cl (Cl/Fe = 0.08). Transformation of akaganéite into more stable phases like goethite or hematite was probably retarded due to the presence of Si and Mn [7-8].

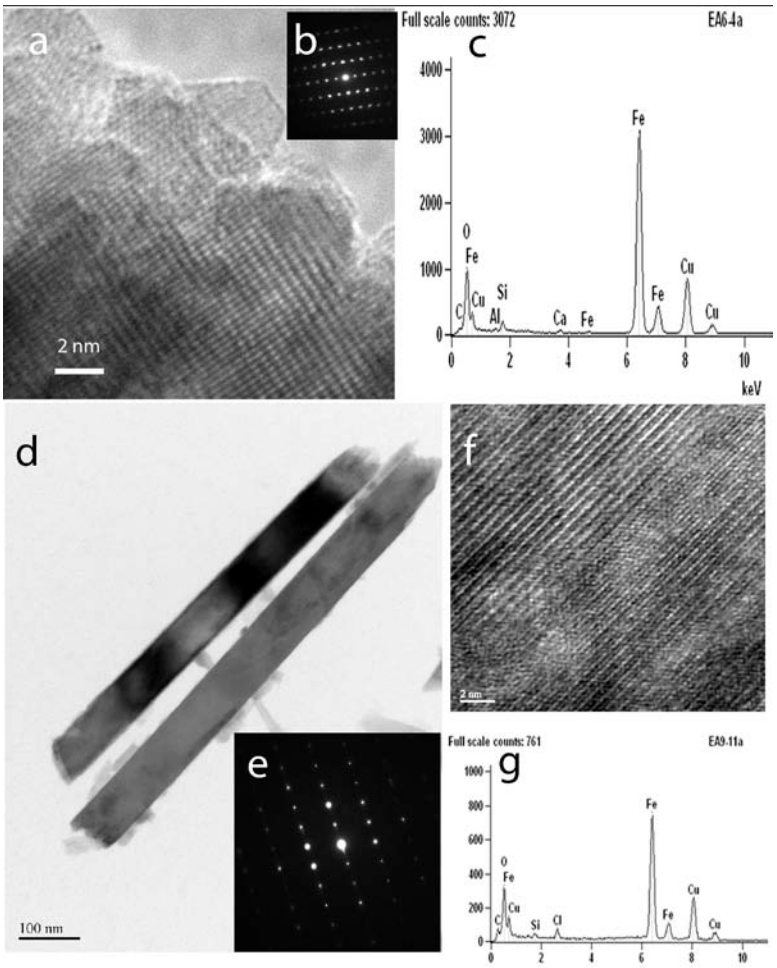

Fig. 6 Akaganéite from Ein Ashlag; a) A high resolution image of akaganéite 3 m from the discharging spring, preserving the morphology of a ferrihydrite precursor; b) An electron diffraction of akaganéite in the image a; c) A point analysis of akaganeite in the image a; d) Rod-shaped akaganéite crystals 10 m from the discharging spring; e) Electron diffraction of akaganéite from the image d; f) A high resolution image of rod-shaped akaganéite; g) A point analysis of rod-shaped akaganéite.

3.5 Lepidocrocite

Lepidocrocite – γ FeOOH (20-100nm) had two morphologies lath-like and an acicular character with some twinning (Figure 7). Impurities in lepidocrocite crystals include Si (Si/Fe= 0.07-0.08), Mg (Mg/Fe = 0.05-0.06), Mn (Mn/Fe = 0.06) and Ca(Ca/Fe = 0.02). The morphology of the crystals reflects changes in oxidation rates, temperature and pH. At slow oxidation rates and at higher temperatures, single laths form and, at faster oxidation rates, the crystals are thinner. Usually lepidocrocite crystallizes at pH > 5 (.) [6]. The appearance of a multi-domain character or twinning occurs at a higher pH [5].

3.6 Hematite

Hematite α-Fe_2O_3 (5-10nm) were observed within the crust in a riverbed, preserving the size and morphology of ferrihydrite (Figure 8a). Impurities within the crystals were Si (Si/Fe=0.38), Mg (Mg/Fe = 0.2), Ca (Ca/Fe = 0.06) and Al (Al/Fe = 0.05). Usually hematite is formed at elevated temperatures by dehydration and rearrangement from a ferrihydrite precursor. This type of transformation could have

occurred in a riverbed due to common elevated temperatures at the Dead Sea area.

The presence of dissolved Si in the Dead Sea brines favors the precipitation of short-range ordered ferrihydrite as an initial phase. All samples had a Si impurity that usually hinders crystal growth. Si impurity within other iron-oxides might result from the brines or from the ferrihydrite precursor. A Mn impurity that was detected in most of the samples might influence the kinetics of transformation and retard it to more stable phases [8]. Precipitation of goethite requires the presence of carbonate whereas akaganéite precipitation requires the presence of Cl. Since precipitation occurred on the surface in changing conditions of weather or spring flow, both phases precipitated. Both phases that were formed by transformation at Ein Ashlag, 10 m from the discharging spring, became more pure than the initial phases. Other impurities that were detected in the iron-oxides result from the composition of the Dead Sea water that is blown at the area as aerosols and the chemical composition of the discharging springs. Another component that contributes to the composition is dust, mainly made of clay minerals and some apatite [9]. P and Zn might be adsorbed on the surfaces of akaganéite and goethite.

Co-precipitation of lepidocrocite, goethite and akaganéite close to each other results from the high concentration of the salinity of the brines that reduces the mobility of iron and oxygen in the brine [5].

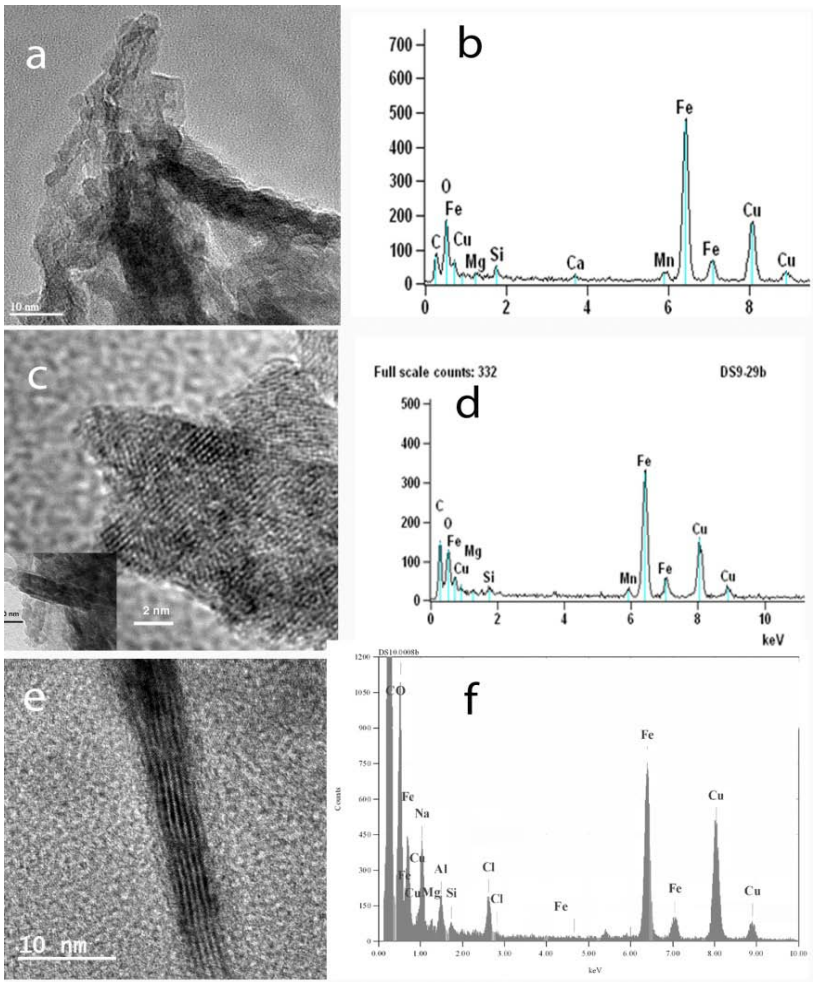

Fig. 7 a, b) Platy lepidocrocite with point analyses; c, d) A high resolution image of lepidocrocite with plate morphology and point analysis; e, f) A high resolution image of rod- shaped lepidocrocite with point analysis.

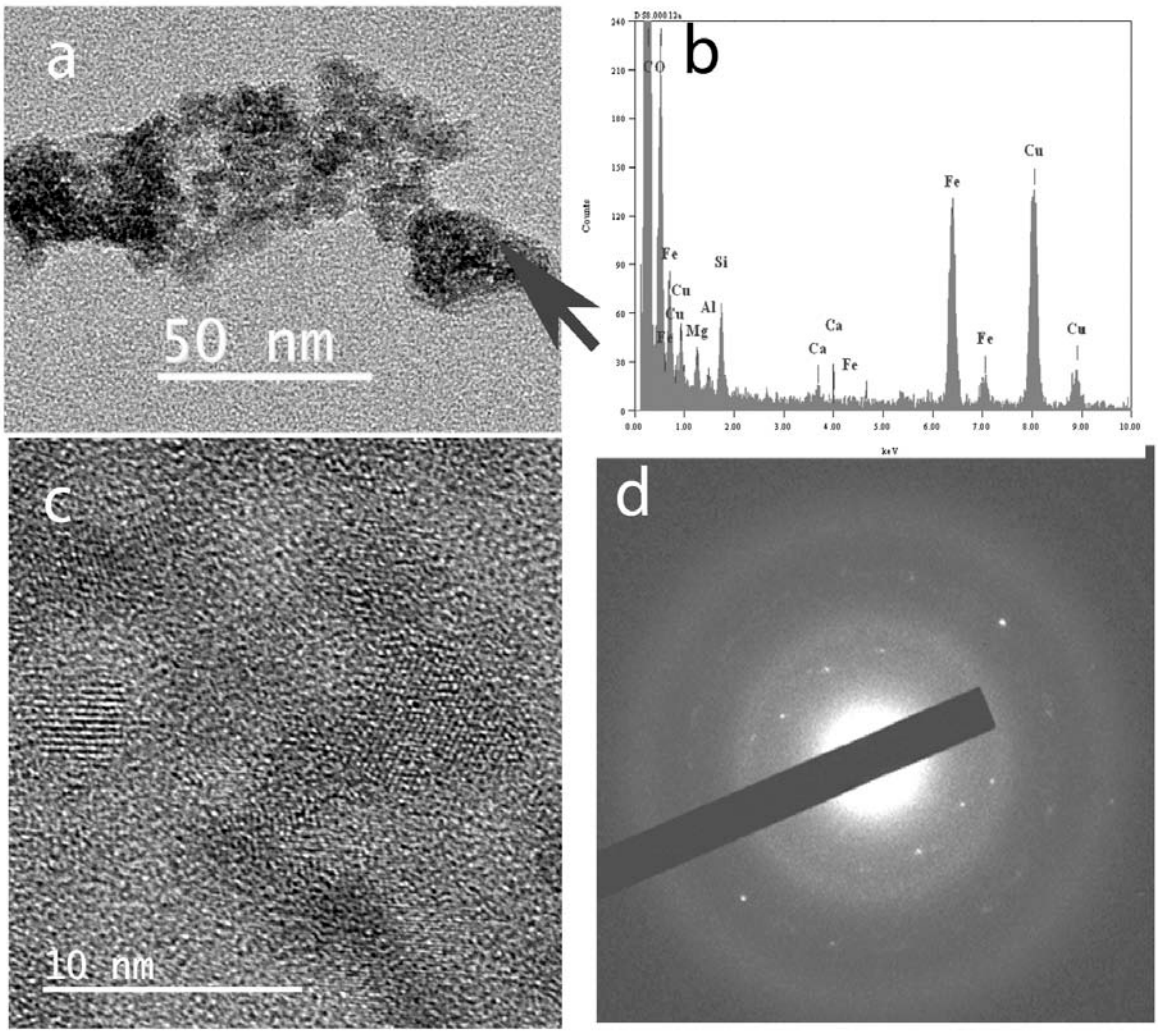

Fig. 8 a) A cluster of nano-sized hematite; b) A point analysis of hematite crystals; c) A high resolution image of hematite preserving ferrihydrite morphology, d) Electron diffraction of hematite crystals.

4. Conclusions

Various phases of iron-oxides crystallize from the discharging brines at the Dead Sea area. The initial phase formed is ferrihydrite that later transforms into akaganéite, lepidocrocite, goethite or hematite depending on the surrounding environment. Recrystallization processes at the initial stage preserve the ferrihydrite precursor and initial impurities of Si, Mn and some P. As recrystallization processes continue, the morphology of the precursor disappears and well-crystallized phases are formed almost without impurities.

Acknowledgements

Thanks to Joseph Harash (The Dead-Sea Works Ltd.) for his help.

Thanks to Janet Ezekiel and Olga Zlatkin for assisting in the performance of the early stages of this research.

References

[1] A. Starinsky, A. Katz, 2014, The story of saline water in the Dead Sea rift—the role of runoff and relative humidity, in: Z. Garfunkel, Z. Ben-Avraham, E. Kagan (Eds.), Dead Sea transform fault system: Reviews Springer Dordrecht Heidelberg, New York, London, 2014, pp. 317-353.

[2] A. Katz , A. Starinski, Geochemical history of the Dead Sea, Aquat. Geochem 15 (2009) 159-194.

[3] Y. Kiro, Y. Weinstein, A. Starinsky, Y. Yechieli, Groundwater ages and reaction rates during seawater circulation in the Dead Sea aquifer, Geochimica at Cosmochimica Acta1 22 (2013) 17-35.

[4] K. Kawamura, A. Nissenbaum, High abundance of low molecular weight organic acids in hyper-saline spring water associated with salt diaper, Organ Geochem 18 (1992) 469-476.

[5] N. Taitel-Goldman, A. Singer, Synthesis ofclay-sized iron-oxides under marine hydrothermal conditions, Clay Minerals 37 (2002) 719-731.

[6] R.M. Cornell, U. Schwertmann, The iron-oxides, Structure, Properties, Occurrence and Uses, Wiley-VCH verlagGMbH & Co. KGaA, Weinheim, 2003, p. 664.

[7] R.M. Cornell, R. Giovanoli, Transformation of akaganéite into goethite and hematite in alkaline media, Clays and Clay Minerals 38 (1990) 469-476.

[8] R.M. Cornell, R. Giovanoli, Transformation of akaganéite into goethite and hematite in the presence of Mn, Clays and Clay Minerals 39 (1991) 144-150.

[9] A. Singer, E. Ganor, S. Dultz, S. Fischer, Dust deposition over the Dead Sea, Journal of Arid Environments 53 (2003) 41-59.